Transition-Metal-Doped p-Type ZnO Nanoparticle-Based Sensory Array for Instant Discrimination of Explosive Vapors

Jiang Qu, Yuru Ge, Baiyi Zu, Yuxiang Li, and Xincun Dou**

The development of portable, real-time, and cheap platforms to monitor ultratrace levels of explosives is of great urgence and importance due to the threat of terrorism attacks and the need for homeland security. However, most of the previous chemiresistor sensors for explosive detection are suffering from limited responses and long response time. Here, a transition-metal-doping method is presented to remarkably promote the quantity of the surface defect states and to significantly reduce the charge transfer distance by creating a local charge reservoir layer. Thus, the sensor response is greatly enhanced and the response time is remarkably shortened. The resulting sensory array can not only detect military explosives, such as, TNT, DNT, PNT, PA, and RDX with high response, but also can fully distinguish some of the improvised explosive vapors, such as AN and urea, due to the huge response reaching to 100%. Furthermore, this sensory array can discriminate ppb-level TNT and ppt-level RDX from structurally similar and high-concentration interfering aromatic gases in less than 12 s. Through comparison with the previously reported chemiresistor or Schottky sensors for explosive detection, the present transition-metal-doping method resulting ZnO sensor stands out and undoubtedly challenges the best.

1. Introduction

The rapid, sensitive, and selective detection of explosives, especially, by employing a portable gas sensor, has been a research focus due to plenty of adverse events, increasing threat of terrorism attack and the need for homeland security.[1] Nitro-explosive is one of the most important categories in common explosives.[2] Rapid detection of the vapors of nitro-explosives is still a challenge due to their low vapor pressure at room temperature, such as, the saturated vapor pressures of 2,4,6-trinitrotoluene (TNT), dinitrotoluene (DNT), para-nitro toluene (PNT), picric acid (PA), and hexogen (RDX) are 9 ppb (part per billion), 411 ppb, 647 ppb, 0.97 ppb, 4.9 ppt (part per trillion), respectively.[3] Besides the nitro-explosives, which are usually named as the military explosives, homemade explosives, which are often referred to as improvised explosives (IEs), are being produced widely by the disparate terrorist groups throughout the world. Ammonium nitrate-fuel oil (ANFO) and urea nitrate (UNi) are two main kinds of IEs.[4] ANFO, the most common explosive produced from ammonium nitrate (AN), is easily made by mixing 94 wt% AN with 6 wt% common diesel fuel. AN contains both a fuel (hydrogen atoms) and an oxidizer (the nitrate group) in the same molecule. Adding a fuel to AN gives the excess oxygen reagent to react with to produce additional energy. UNi, with the chemical formula NH_2CONH_2–HNO_3, is made by mixing nitric acid with urea,

J. Qu, Y. R. Ge, Dr. B. Y. Zu, Y. X. Li, Prof. X. C. Dou
Laboratory of Environmental Science and Technology
Xinjiang Technical Institute of Physics & Chemistry;
Key Laboratory of Functional Materials and
Devices for Special Environments
Chinese Academy of Sciences
Urumqi 830011, China
E-mail: byzu@ms.xjb.ac.cn; xcdou@ms.xjb.ac.cn
J. Qu
University of Chinese Academy of Sciences
Beijing 100049, China

DOI: 10.1002/smll.201503131

and one molecule of urea attaches to one molecule of nitric acid. In this explosive, urea and nitric acid serve as the fuel and the oxidizer, respectively. UNi can be transformed into nitrourea ($NH_2CONH–NO_2$), a more powerful explosive, through the process of dehydration (chemical removal of water).[4] Therefore, the detection of IEs (ANFO, UNi, and nitrourea) can be achieved based on the indirect detection of their raw materials like AN and urea. Currently, most of the operational equipment for explosive detection are either expensive or bulky, such as, ion mobility spectrometer,[5] mass spectrometer,[6] and surface-enhanced Raman spectroscopy.[7] Therefore, the development of portable, real-time, and cheap platforms to monitor ultratrace level of explosives is of great urgence and importance.

ZnO-based gas sensors have been applied in many fields to detect trace analytes, such as, ethanol,[8] urea,[9] and TNT.[10] A ZnO nanorod-based chemiresistor sensor shows good sensitivity toward trace (down to few ppb) DNT and TNT molecules.[11] However, the most leading ZnO nanostructure-based chemiresistor explosive sensors only have limited responses, such as, 20% toward 60 ppb TNT vapor.[10] It is proposed that the surface defect states on metal oxides play an extremely important role in enhancing the chemisorption of analyte molecules.[12] Thus, the intentional creation of surface defect states on ZnO might remarkably enhance the chemisorption ability of ZnO and the response value of the sensor. On the other hand, the response speed of the previous chemiresistor explosive sensors is far from the practical application, for example, a ZnO nanowire-based sensor shows a response time of 10 min.[10] Thus, the development of a new method to significantly reduce the response/recovery time would be of vital importance. It is well known that the response time of a sensor is highly related to the charge exchange rate between the sensing materials and the adsorbed target molecules.[13] Transition-metal-doping can significantly improve the mobility of charge carriers by introducing impurity energy band states.[14] However, none of the previous works focus on improving the response speed by employing the transition-metal-doping method, which is of extremely vital importance for practical real-time detection.

Herein, we present a transition-metal-doping method to remarkably promote the quantity of the surface defects states and to create a local charge reservoir layer in p-type ZnO nanoparticles. The resulting transition-metal-doped ZnO nanoparticle-based chemiresistor gas sensory array exhibits ultrahigh responses toward room-temperature saturated vapors of nitro-explosives (TNT, DNT, PA, PNT, and RDX), AN, and urea. It is found that singly ionized oxygen vacancy plays a decisive role in the sensor response promotion. Furthermore, this sensory array can realize the discrimination of TNT and RDX from structurally similar interfering aromatic gas molecules (benzene, toluene, and nitrobenzene) with a high concentration in less than 12 s. The fast response can be attributed to the accelerated charge exchange rate with the adsorbed target molecules by transition-metal-doping. The proposed sensing materials designing concept and the resulting sensory array analysis method are highly promising in the realization of portable, real-time, and cheap platforms for ultratrace levels of explosive monitoring.

2. Results and Discussion

2.1. Singly Ionized Oxygen Vacancy ($V_O^{\bullet}$) Determined Response of Fe-Doped ZnO Nanoparticle-Based Chemiresistor Sensor

Scanning electron microscopy (SEM) characterization (**Figure 1**a) shows the nanoparticles morphology of the prepared Fe-doped ZnO (Fe-ZnO), with a diameter ranging from 5 to 50 nm. It is expected that this broad particle size distribution of the Fe-ZnO nanoparticles is beneficial to improve the sensitivity and stability of the resulting gas sensor due to the boundary-neck-grain simultaneously controlled sensing mechanism.[15] The Fe-ZnO nanoparticles were formed from nanosheets after an annealing process at 400 °C for 1 h (Figure S1a,b, Supporting Information). High-resolution transmission electron microscopy (HRTEM) image shows that the lattice space of 0.291 nm can be well corresponded to the (100) direction of wurtzite ZnO (Figure 1b). All the X-ray diffraction (XRD) peaks are sharp and can be well assigned to powder phase wurtzite ZnO (JCPDS, 36–1451), proving the pure phase of the obtained Fe-ZnO nanoparticles and there is no significant mismatch comparing with the ZnO nanoparticles without doping (Figures S1c and S2a–c, Supporting Information). The peak located at an energy of 6.4 KeV in the Energy disperse spectroscopy (EDS) spectra (Figure S1d, Supporting Information), which corresponds to the Kα transition and forms a sharp contrast with the ZnO nanoparticles (Figure S2d, Supporting Information), clearly demonstrates the existence of Fe in the final product, and the atomic ratio of Fe is 6.8%. The energy peak located at 711.0 eV in the X-ray photoelectron spectroscopy (XPS) spectra represents the binding energy of Fe 2p in Fe_2O_3 (Figure 1c), indicating the successful doping of Fe in the site of Zn. Capacitance–voltage (C–V) measurement was applied to determine the conduction type of the sensing material. It is known that in the Mott-Schottky (MS) plots, a positive slope represents an n-type behavior, while a negative slope points to a p-type behavior.[16] It is clearly shown that both ZnO and Fe-doped ZnO nanoparticles in this study are p-type semiconductors (Figure 1d and Figure S2e, Supporting Information).

It is known that the surface defect states on metal oxides play an extremely important role in enhancing the chemisorption of the analyte molecules. To investigate the category and the quantity of the surface defects, EPR (Electron Paramagnetic Resonance) spectrometer was adopted to analyze the features of the related surface defects. From the EPR investigation (Figure 1e), it is observed that there is a main resonance line in the spectra located at a magnetic field strength of 3445 G, which corresponds to the electron's so-called g-factor of around 1.96 (calculation details shown in the Supporting Information), and it can be attributed to the unpaired electrons trapped on oxygen vacancies (singly ionized oxygen vacancy $V_O^{\bullet}$).[17] It is shown that the annealing temperature has a significant influence on the peak intensity of $V_O^{\bullet}$ defects. With the annealing temperature of 200 °C, the EPR intensity of $V_O^{\bullet}$ is around 170. When the annealing temperature increases to 400 °C, the EPR intensity increases to

DOI: 10.1002/smll.201503131

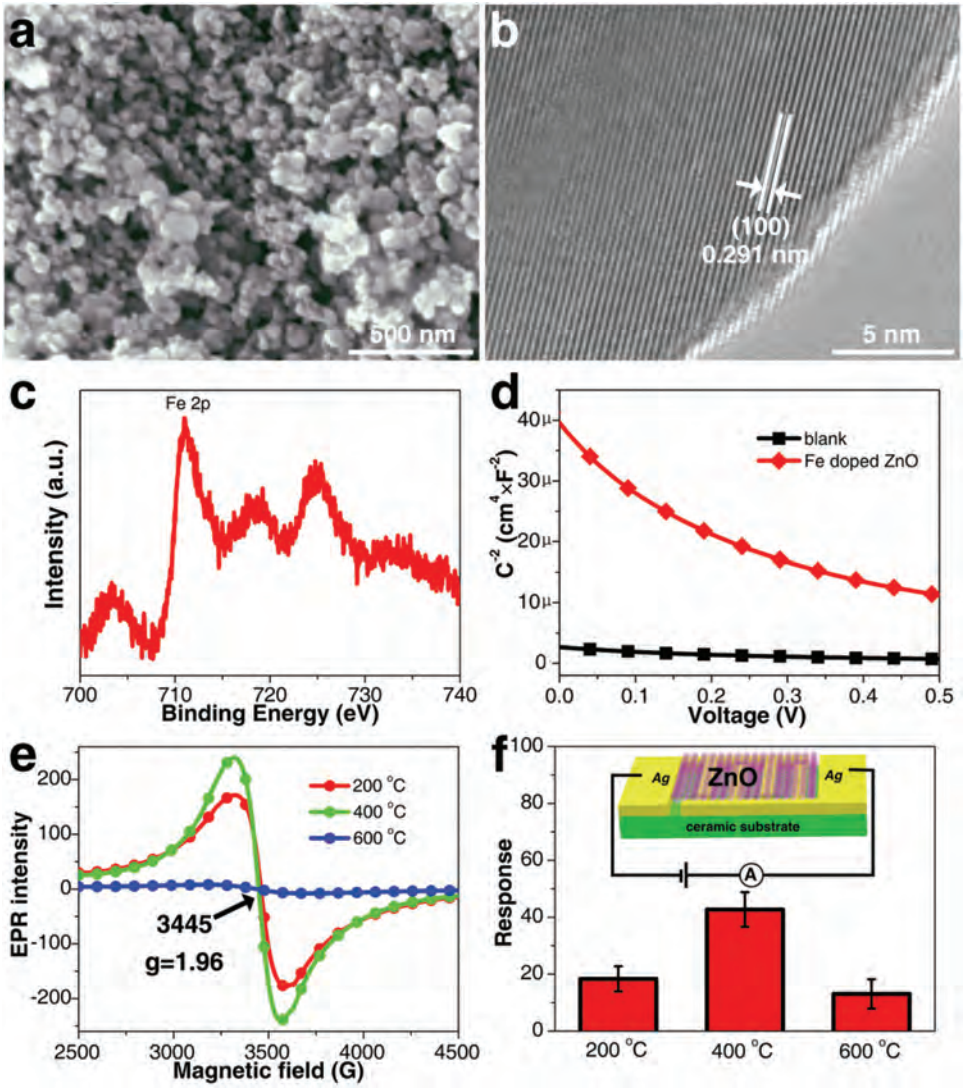

Figure 1. a) FESEM, b) TEM image, and c) XPS of the Fe 2p peak of Fe-ZnO nanoparticles d) Mott-Schottky plots of Fe-ZnO nanoparticles and the blank substrate, e) the EPR spectrum comparison of Fe-ZnO after heat treatment at 200, 400, and 600 °C for 1 h, and (f) the corresponding responses of the sensors toward room-temperature (25 °C) saturated vapor of TNT; inset is the schematic graph of the sensor structure.

240. With a further increase of the annealing temperature to 600 °C, the EPR intensity decreases to 8. Thus, the selection of the annealing temperature has a decisive role in controlling the quantity of defects.

To further investigate how the singly ionized oxygen vacancies exactly influence the sensor sensitivity, the corresponding sensing performances of the sensors (the device structure is shown by the inset in Figure 1f) fabricated with Fe-ZnO nanoparticles annealed at different temperatures were evaluated at room temperature (25 °C) toward saturated TNT vapor. The detailed measurement setup is shown in Scheme S1. From the resistance change behavior (Figure S3, Supporting Information), it is clearly shown that with the immersing of the sensor into TNT vapor, the resistance decreases rapidly, and with the immersing of the sensor into air, the resistance increases fast and can recover to the initial value, indicating the good repeatability of the sensor. It is considered that with the chemisorption of the electron-deficient gas, such as TNT vapor, the aromatic ring and three electron-withdrawing nitro groups can strongly bind the TNT molecules onto the surface of Fe-ZnO nanoparticles.[18] Thus, more holes will be generated and the resistance will be decreased due to the p-type behavior of the Fe-doped ZnO nanoparticles. From the response values of the three sensors (Figure 1f), it can be observed that the sensor response shows a maximum value at 400 °C. Furthermore, the response values of these three sensors correspond well with the quantity of the $V_O^{\bullet}$ defects, that is, the larger the quantity of the $V_O^{\bullet}$ defects, the higher the response value. Thus, it can be concluded that the amount of $V_O^{\bullet}$ centers plays a decisive role in the sensor response since the increase/decrease of the corresponding EPR peak could cause an increase/decrease in the sensor response.

To further verify the decisive role of the quantity of $V_O^{\bullet}$ centers on the sensor response, the EPR spectra of different temperatures annealed ZnO nanoparticles without Fe doping were measured and the corresponding sensor responses toward TNT vapor were evaluated and compared. It is also

shown that at an annealing temperature of 200 and 400 °C, the EPR peak representing $V_O^{\bullet}$ centers can also be observed (Figure S4, Supporting Information), and the resulting sensors show responses of 13.2% and 26.4% (Figure S5, Supporting Information). However, at an annealing temperature of 600 °C, the EPR peak can be observed is chaotic and the resulting sensor has no response toward TNT. Furthermore, it is found that the commercial ZnO powder has no EPR peak and the corresponding sensor has no response toward TNT vapor (Figure S4, Supporting Information). These results further illustrate that the amount of $V_O^{\bullet}$ centers, which closely relating to the annealing temperature, plays a decisive role in the sensor response.

2.2. Rapid Detection toward Military and Improvised Explosive Vapors

To systematically investigate the gas sensing performance of the Fe-doped ZnO nanoparticle-based sensor, six military explosive vapors (TNT, TNT (purified), DNT, PA, PNT, and RDX) and two improvised explosive vapors (AN and urea) saturated at room temperature were used as the testing gases, respectively. Three successive cycles were measured and compared with the response changes of the ZnO nanoparticle-based sensor (**Figure 2**a and Figure S6 in the Supporting Information). It can be easily observed that the responses of the Fe-doped ZnO nanoparticle-based sensor are almost the same with those of the ZnO nanoparticle-based sensor toward a certain explosive vapor. Furthermore, both sensors show much higher responses toward AN and urea comparing to those of nitro-explosives (≈100% vs 18.2–44.6%), which can be attributed to the dissociation of solid AN (with a gas concentration at 6.79 ppb[19]) into NH_3 and HNO_3 at 25 °C[20] and the decomposition of urea into HNCO and NH_3.[21]

The schematic diagrams of the response changes of ZnO and Fe-ZnO nanoparticle-based sensors, which are deduced from the response changes in Figure 2a, clearly show that the Fe-ZnO nanoparticle-based sensor can respond to saturated explosive vapors and air much more rapidly compared to the ZnO nanoparticle-based sensor (Figure 2b). As shown in Figure 2c,d, the Fe-doped ZnO nanoparticle-based sensor shows a much faster response and recovery process toward all of the saturated explosive vapors, especially, both the response time and recovery time toward saturated nitro-explosive vapor are less than 10 s, which are in sharp contrast with those of the ZnO nanoparticle-based sensor (>25 and >30 s). It should be pointed out that the response time and the recovery time of the Fe-doped ZnO nanoparticle-based sensor toward AN and urea are less than 10 and 30 s, respectively, regardless the large response. This result clearly indicates that Fe-doping is an effective strategy to shorten the sensor response time and thus plays a decisive role in boosting the whole performance of the sensing device. Besides, our preliminary results have partly shown that the real-time sensing toward vapors of nitro-explosives and improvised explosives could be realized by transition-metal-doping, such as, Fe-doping.

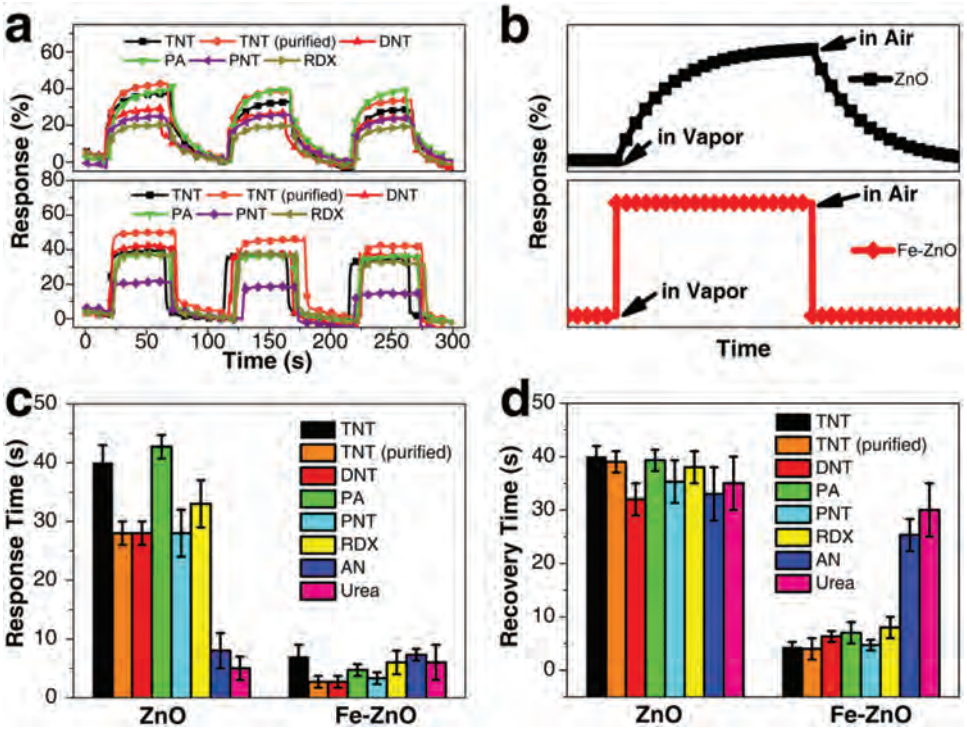

Figure 2. a) Response changes of two sensors based on ZnO (up) and Fe-ZnO (down) nanoparticles during three successive cycles of exposure to TNT, TNT (purified), DNT, PA, PNT, and RDX vapors (25 °C), b) schematic diagram of the response changes of ZnO (up) and Fe-ZnO (down) nanoparticle-based sensors. Comparison of c) the response time and d) the recovery time of the two sensors based on ZnO and Fe-ZnO nanoparticles toward room-temperature saturated vapors of TNT, TNT (purified), DNT, PA, PNT, RDX, AN, and urea.

small 2016,
DOI: 10.1002/smll.201503131

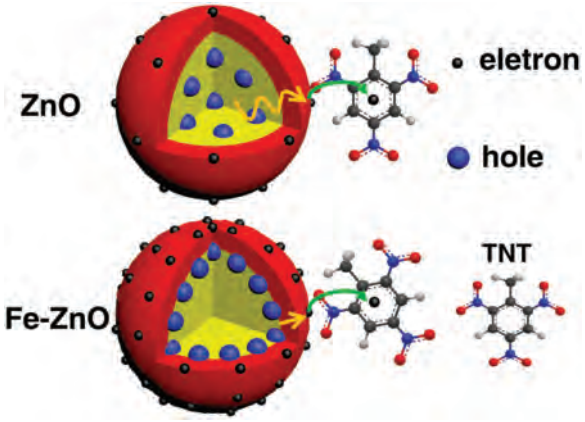

Figure 3. Two models of charge transfer in a nanoparticle: up, the charge is transferred from the body of the particle to the surface in ZnO nanoparticles, whereas down, the charge is transferred from the local charge reservoir layer to the surface in Fe-doped ZnO nanoparticles.

2.3. Theoretical Analysis of the Rapid Responding Mechanism

It is generally considered that the sensing function of nanoparticles is dominated by the surface shell, namely the depletion layer, rather than the core area. There is a homogeneous distribution of the charge carriers in the whole core area of a p-type ZnO nanoparticle without Fe-doping (the up part in **Figure 3**). However, the holes would aggregate at the outer surface of the core part in a Fe-doped ZnO nanoparticle, forming a local charge reservoir layer (the bottom part in Figure 3).[22] Thus, the charge transfer distance from the core part to the surface defects centers in a Fe-doped ZnO nanoparticle is greatly reduced compared to the non-doping counterpart. As a result, once a target electron-withdrawing molecule, such as a TNT molecule, adsorbs on the surface defect center and transfers one electron from the particle surface to the target molecule, the electrons in the core part would feed to the surface shell immediately. Apparently, the Fe-doped ZnO nanoparticle could finish this local response more rapidly. At the same time, as can be evidenced by the nearly fixed response values between the two kinds of ZnO nanoparticles, the total number of the absorbed electrons on the sensing film is certain due to the low vapor pressure of the target analytes. Thus, the total time consumed for the electrical signal change caused by the charge transfer to the target analyte, namely the response time, is greatly shortened by Fe-doping.

2.4. Transition-Metal-Doping: A General Strategy to Shorten the Sensor Response Time

In order to further illustrate that transition-metal-doping could be a general strategy to shorten the sensor response time, two other transition metals, cobalt and nickel, are selected as the doping elements of ZnO to evaluate the sensing performance of the doped ZnO (Co-ZnO and Ni-ZnO) sensors. Both Co-ZnO and Ni-ZnO nanostructures annealed at 400 °C for 1 h were characterized by SEM and confirmed to be nanoparticles with a diameter ranging from 5 to 50 nm (**Figure 4**a,d). XRD characterization shows that both samples are pure phase wurtzite ZnO (Figure S7a, Supporting Information). The room-temperature EPR spectrum show that $V_O^{\bullet}$ centers could be obviously observed in both Co-ZnO and Ni-ZnO nanoparticles, and the intensity of them are 0.3 and 2, respectively (Figure 4b,e). EDS spectra show that the atomic ratios of Co and Ni are 2.2% and 2.1%, respectively (Figure S7b, Supporting Information). The energy peaks located at 780.1 eV and 853.6 eV in the XPS spectra represents the binding energy of Co 2p and Ni 2p, respectively (Figure 4c,f), suggesting the successful doping of Co or Ni in the final product.

The sensing performance of both Co-ZnO and Ni-ZnO nanoparticle-based sensors toward six military explosive vapors and two improvised explosive vapors was also evaluated at room temperature. All the dynamic response changes of both sensors for three successive cycles are shown in Figure S8 (Supporting Information), in which one can see the good repeatability of both sensors. The statistical response values are shown in Figure 4g, in which one also can see that both sensors exhibit much higher responses toward AN and urea comparing to those of nitro-explosives. Thus, it is considered that the present transition-metal-doped nanoparticle-based sensors can well detect AN and urea due to the corresponding large and specific responses. Both sensors show a response time of less than 12 s toward all the explosive vapors and the recovery time toward saturated nitro-explosive vapors are less than 10 s (Figure 4h,i). Thus, it is further confirmed that transition-metal-doping is an effective strategy to shorten the sensor response time and recovery time. It is concluded that the rapid gas sensing performance can be attributed to the existence of a local charge reservoir layer resulting from transition-metal-doping.

The comparison of the performance (including the sensor response, response time, and recovery time) of the present transition-metal-doped ZnO nanoparticle-based sensors and other recently reported chemiresistor or Schottky sensors toward explosive vapors detection can be found in **Table 1.** It is clearly shown that the present transition-metal-doped ZnO nanoparticle-based sensors belong to the best TNT and DNT sensors since the responses toward them are 45.5% and 38.9%, respectively, and are comparable to the best titania (B) nanowires-based chemiresistor gas sensor (47% for TNT[23] and 38% for DNT[27]). The responses for PA and RDX are 36.1% and 45.5%, which are much higher than those of the best Schottky sensor based on SiNWs array/TiO_2/rGO junction (4% for PA and 9% for RDX).[27] What is more, all the response time and recovery time for TNT, DNT, PA, PNT, and RDX are less than 8 s, which is remarkably superior than all of the other sensors.[10,25–27] This comparison further confirms that the present transition-metal-doping method could be a very promising strategy to put the nanomaterials-based explosive sensors into practical application.

2.5. Rapid Response toward High-Concentration Volatile Organic Compounds by the Transition-Metal-Doped ZnO Nanoparticle-Based Sensors

It is known that the response time of a sensor is closely related to the sensor response, that is, a higher response

DOI: 10.1002/smll.201503131

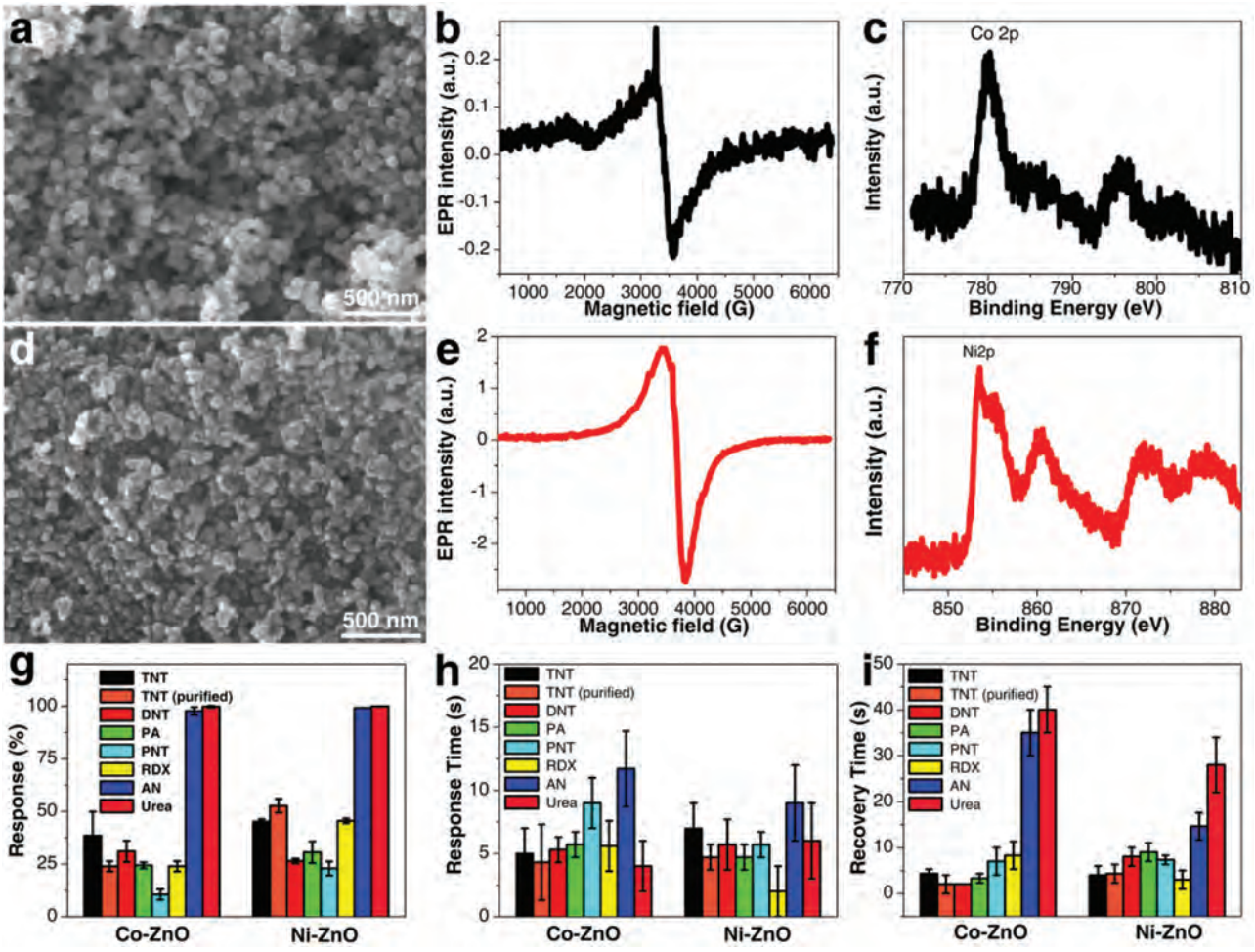

Figure 4. a) FESEM image, b) EPR intensity, and c) XPS of Co 2p peaks of the Co-ZnO nanoparticles, d) FESEM image, e) EPR intensity, and f) XPS of Ni 2p peaks of the Ni-ZnO nanoparticles. Comparison of the g) gas responses, h) response time, and i) recovery time of the two sensors based on Co-ZnO and Ni-ZnO nanoparticles toward room-temperature saturated vapors of TNT, TNT (purified), DNT, PA, PNT, RDX, AN, and urea.

usually relates to a longer response time due to the slow adsorption of the target gas molecules. Thus, the concentration of the target gas, which highly related to the adsorption process, plays a crucial role in evaluating the response time of a sensor. Herein, high level volatile organic compounds, such as benzene (12.53%), toluene (3.85%), and nitrobenzene (394.7 ppm) (the detailed calculation process is described in the supporting information) are chosen to evaluate the performance of the three transition-metal-doped ZnO nanoparticle-based sensors.

The dynamic response change of the three sensors toward benzene, toluene and nitrobenzene with three successive cycles are compared with those of the ZnO nanoparticle-based sensor, respectively (Figure S9, Supporting Information). It is observed that all of the four sensors show a good repeatability. Besides, the response values are ranging from 22.3% to 75.3%, and there is no obvious variation in response from sensor to sensor (**Figure 5**a). Remarkably, it is found that all the response time of the three transition-metal-doped ZnO nanoparticle-based sensors, ranging from 1.3 to 13 s, are significantly shorter than that of the ZnO nanoparticle-based sensor (5.3–22 s). Furthermore, the recovery time is also greatly shortened with the transition-metal-doping (1.3–11.7 s vs 17.3–24 s) (Figure 5b). This result clearly demonstrates that transition-metal-doping definitely is an effective strategy to improve the response speed and the recovery process of a sensor even toward high-concentration target gas detection. This fast react process can be definitely attributed to the efficient formation of a local charge reservoir layer by transition-metal-doping.

2.6. Instant Discrimination of Nitro-Explosives from Structurally Similar High-Concentration Interfering Gases with the Transition-Metal-Doped ZnO Nanoparticle-Based Sensory Array

To verify whether the present sensors can rapidly realize the function of discriminating explosive vapors from the common interfering gases, the above three transition-metal-doped ZnO nanoparticle-based sensors were made into a sensory array (**Figure 6**a). Principal component analysis (PCA) method is adopted to analyze the responses toward typical nitro-explosives (TNT and RDX) and the structurally similar high level volatile organic compounds (Figure S10, Supporting Information). It is shown that the clusters representing TNT

DOI: 10.1002/smll.201503131

small NANO MICRO

Table 1. Comparison of different gas-phase nitro-explosive sensors and the present transition-metal-doped ZnO nanoparticle-based sensors

Sensing materials	Analytes' concentration	Response	Response time	Recovery time	Ref.
ZnO nanowire	TNT 60 ppb	20%	>10 min	–	[10]
SWNT	TNT, 8 ppb	8%			
Titania(B) nanowires	TNT, 9 ppb	47%	≈5 s	≈5 s	[23]
	DNT, 180 ppb[a)]	38%			
Organic nanoribbons	4-PNT 100 ppm	15%	<5 s	>100 s	[24]
	DNT 100 ppb	40%			
SXFA-coated microcantilevers	DNT 300 ppt	–	35 s	35 s	[25]
GaN/TiO_2 NWNC hybrids	TNT, 100 ppb	10%	30	–	[26]
	DNT, 100 ppb	2%			
SiNWs array/TiO_2/rGO	TNT 9.1 ppb	6.3%	≈80 s	≈75 s	[27]
	DNT 411 ppb[b)]	40%	≈120 s	≈80 s	
	PNT 647 ppb	56%	≈75 s	≈150 s	
	PA 0.97 ppb	4%	≈70 s	≈100 s	
	RDX 4.9 ppt	9%	≈30 s	≈75 s	
Ni-ZnO	TNT 9.1 ppb	45.5%	≈4.3 s	≈4 s	This work
Fe-ZnO	DNT 411 ppb[b)]	38.9%	≈5.3 s	≈6.3 s	
Ni-ZnO	PNT 647 ppb	22.9%	≈5.7 s	≈7.3 s	
Fe-ZnO	PA 0.97 ppb	36.1%	≈4.7 s	≈7 s	
Ni-ZnO	RDX 4.9 ppt	45.5%	≈2 s	≈3 s	

[a)] The room-temperature saturated vapor pressure of DNT from ref. [28]; [b)]The room-temperature saturated vapor pressure of DNT from refs. [3a],[29].

and RDX aggregate separately and are far from each other and the interfering gases clusters (Figure 6b). Herein, PC 1 and PC 2 account for 67.08% and 32.92% of the data variance, respectively. Thus, this transition-metal-doped ZnO nanoparticle-based sensory array can well recognize 9.1 ppb TNT and 4.9 ppt RDX from 12.5% benzene, 3.85% toluene and 394.7 ppm nitrobenzene in less than 13 s.

Furthermore, it is known that with the increase of the sensor number in a sensory array, the discriminating capability of the sensory array toward different target gases could be further promoted. Thus, all the four sensors in this study were organized into a sensory array (Figure 6c) and from the PCA plot one can see that all the nitro-explosives can be recognized from those interfering aromatic-compounds (Figure 6d).

3. Conclusion

In summary, a transition-metal-doping method is first introduced to remarkably promote the quantity of the surface defect states and to create a local charge reservoir layer in p-type ZnO nanoparticles. The resulting transition-metal-doped ZnO nanoparticle-based chemiresistor gas sensory array shows ultrahigh responses toward room-temperature saturated vapors of nitro-explosives and the vapors of two improvised explosives. The quantity of singly ionized oxygen vacancy plays a decisive role in the sensor response promotion. Most importantly, the response time and the recovery time of the sensors fabricated by transition-metal-doped ZnO nanoparticles are greatly shortened. Typically, all the response time toward TNT, DNT, PNT, PA, RDX, AN, and

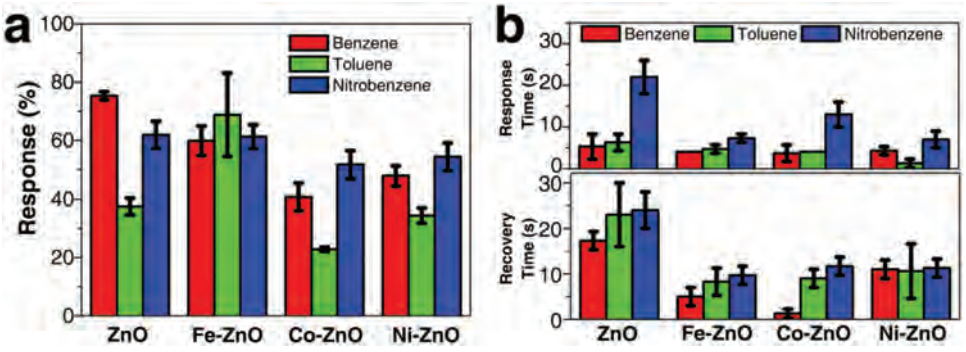

Figure 5. a) Responses of four sensors based on ZnO, Fe-ZnO, Co-ZnO, and Ni-ZnO nanoparticles exposing to benzene, toluene, and nitrobenzene; (b) comparison of the corresponding response time (up) and recovery time (down) of the four sensors.

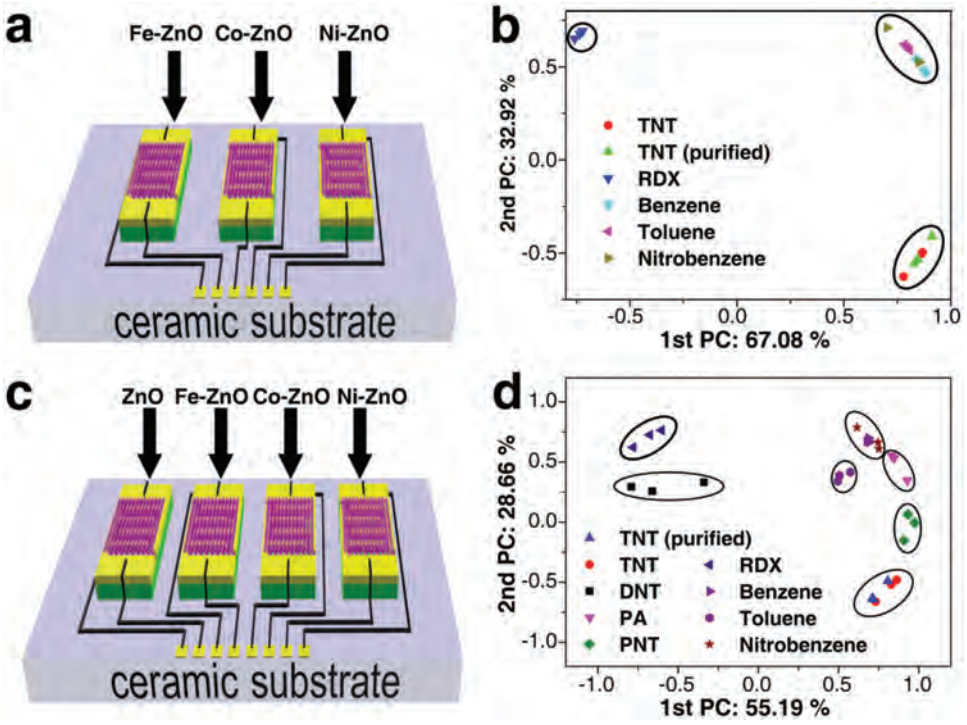

Figure 6. a) Schematic diagram of a gas sensory array composed of three doped sensors based on Fe-ZnO, Co-ZnO, and Ni-ZnO nanoparticles; (b) the corresponding PCA of sensing response to different analytes; (c) schematic diagram of a gas sensory array composed of four sensors based on ZnO, Fe-ZnO, Co-ZnO, and Ni-ZnO nanoparticles; d) the corresponding PCA of sensing response to different analytes.

urea are reduced to less than 12 s, and all the recovery time toward the nitro-explosives are shorter than 10 s, making these transition-metal-doped ZnO nanoparticle-based sensors extremely applicable for practical real-time detection. Furthermore, this sensory array can realize the discrimination of ppb-level TNT and ppt-level RDX from structurally similar and hundreds ppm above interfering aromatic gases in less than 13 s. This fast react process is originated from the efficient formation of a local charge reservoir layer by transition-metal-doping. Thus, the present transition-metal-doping method to boost the sensor performance presents a totally new understanding in the underlying mechanisms influencing the sensor performance by a systematical analysis on the surface defects and the structure of the sensing material. We expect that this study would shine light on the realization of portable, real-time, and cheap platforms for ultratrace levels of explosive monitoring.

4. Experimental Section

Chemicals and Reagents: Commercial ZnO powder, Zincnitrate hydrate ($Zn(NO_3)_2{\cdot}6H_2O$), Ferric nitrate nonahydrate ($Fe(NO_3)_3{\cdot}9H_2O$), Cobalt nitrate tetrahydrate ($Co(NO_3)_2{\cdot}4H_2O$), Nickel acetate tetrahydrate ($Ni(CH_3COO)_2{\cdot}4H_2O$), Lithium hydroxide monohydrate ($LiOH{\cdot}H_2O$), absolute ethanol, heptane, DNT, PNT, PA, AN, and urea were purchased from Sigma-Aldrich. Raw TNT and RDX were obtained from the National Security Department of China and simplified as TNT and RDX in the text. Except for TNT was recrystallized with ethanol before use and labeled as TNT (purified), all the other explosives were used directly without further purification.

Caution: TNT and other nitro-explosives used in this study are highly explosive and should be handled only in small quantities.[30]

Preparation of Transition-Metal-Doped p-Type ZnO Nanoparticles: The transition-metal-doped p-type ZnO nanoparticles (M-ZnO, where M represents the doped transition metal) were prepared mainly by two steps, a preparation of transition-metal-doped ultrathin nanosheets and a post-annealing process. In a typical procedure, a mixture ethanol solution of 50 mL of 0.1 M $Zn(NO_3)_2{\cdot}6H_2O$ and 0.005 M $M(CH_3COO)_2{\cdot}nH_2O$ or $M(NO_3)_2{\cdot}nH_2O$ (n is the number of crystal water), and an ethanol solution of 50 mL of 0.15 M $LiOH{\cdot}H_2O$ were kept in a refrigerator and maintained at 0 °C separately. Then, the two solutions were mixed together, kept in an ice bath and stirred for 2 h. After that, the precipitation was washed with heptane and ethanol in sequence and repeated three times, finally dried in oven overnight at 60 °C to get the transition-metal-doped ultrathin nanosheets. For the second step, the nanosheets were annealed for 1 h at different temperatures (200, 400 or 600 °C). Pristine ZnO nanosheets were prepared without adding $M(CH_3COO)_2{\cdot}nH_2O$ or $M(NO_3)_2{\cdot}nH_2O$ in the initial process.

Characterization: XRD measurement was conducted using powder XRD (Bruker D8 Advance, with Cu Kα radiation operating at 40 kV and 40 mA, scanning from $2\theta = 10°$ to 90°). Field-emission scanning electron microscope (FESEM, ZEISS SUPRA 55VP) and transmission electron microscope (JEM-2011 TEM, 200 kV) were used to characterize the morphology of the samples. EDS and XPS (Thermo Scientific Escalab 250) were used to quantitatively evaluate the composition of the impurity element in the M-ZnO nanoparticles. EPR spectra were recorded on a Bruker Elexsys E500 spectrometer by applying an X-band (9.43 GHz, 1.5 mW) microwave with sweeping magnetic field at room temperature in cells that can be connected to a conventional high-vacuum apparatus

DOI: 10.1002/smll.201503131

(residual pressure $<10^{-4}$ mbar). The MS plot was recorded by the electrochemical workstation (Zennium Workstation, ZAHNER, Germany), using the ac impedance method. The measurement was conducted in a conventional three-electrode cell, using a ceramic/Ag electrode with ZnO or M-ZnO nanoparticles on the surface, a standard saturated Ag/AgCl and a Pt wire as the working, reference, and counter electrodes, respectively. To measure the MS plot of ZnO or M-ZnO nanoparticles, the amplitude of the ac potential was set at 10 mV, the frequency was 1 kHz, and the electrolyte solution contained 0.1 M Na_2HPO_4 with pH adjusted to 10 by 4 M NaOH.

Gas Sensor Fabrication, Test and Electric Signal Analysis: Initially, the ZnO or M-ZnO nanoparticles were mixed with absolute ethanol in a weight ratio of 100:25 and ground in a mortar for 15 min to form a paste. The paste was then coated on a ceramic substrate by a thin brush to form a sensing film on which silver interdigitated electrodes with both finger-width and inter-finger spacing of about 200 μm were previously printed. The thickness of the film was controlled by the brushed cycles. The sample was dried naturally in air overnight. The sensors were aged at 4 V in air for about 24 h to ensure the good stability since this procedure can greatly reduce the defects amount and improve the grain boundary contact. The room temperature saturated explosive vapor was obtained by putting solid explosive powder at the bottom of a conical flask (250 mL) and sealed for 48 h. Then the sensor was placed into the conical flask shielded with aluminum foil. For gas sensing test, the sensor was inserted into the saturated vapor of an explosive. After the sensor resistance reached a new constant value, the sensor was then inserted into a same size conical flask full of air to recover. The electric signal of the sensor was measured by a Keithley 2636B SourceMeter. The relative sensor response in resistance is defined as, Response $=(R_a - R_g)/R_a \times 100\%$, where R_a and R_g are the electrical resistances of the sensor in air and in explosive vapor. The response time is defined as the period in which the sensor resistance reaches 90% of the response value upon exposure to the explosive vapor, while the recovery time is defined as the period in which the sensor resistance changes to 10% of the response value after the explosive vapor is removed.

Supporting Information

Supporting Information is available from the Wiley Online Library or from the author.

Acknowledgements

The authors thank the financial support from the Research Program of Chinese Academy of Sciences (CAS, CXJJ-16M122), National Natural Science Foundation of China (51201180, 51372273, 51572292), Xinjiang International Science & Technology Cooperation Program (20156005), Xinjiang Program of Cultivation of Young Innovative Technical Talents (2014731020, 2013711015), Xinjiang Program of Introducing High Level Talents, "Hundred Talents Program" of CAS and SRF for ROCS, SEM.

[1] A. Rose, Z. Zhu, C. F. Madigan, T. M. Swager, V. Bulović, *Nature* **2005**, *434*, 876.
[2] S. S. Nagarkar, B. Joarder, A. K. Chaudhari, S. Mukherjee, S. K. Ghosh, *Angew. Chem., Int. Ed.* **2013**, *125*, 2953.
[3] a) J. E. Brady, J. L. Smith, C. E. Hart, J. Oxley, *Propellants, Explos. Pyrotech.* **2012**, *37*, 215; b) L. Senesac, T. G. Thundat, *Mater. Today* **2008**, *11*, 28.
[4] K. Yeager, *Dangerous Innovations*, John Wiley & Sons, Hoboken, NJ **2006**.
[5] S. Cheng, W. Wang, Q. Zhou, C. Chen, L. Peng, L. Hua, Y. Li, K. Hou, H. Li, *Anal. Chem.* **2014**, *86*, 2687.
[6] N. L. Sanders, S. Kothari, G. Huang, G. Salazar, R. G. Cooks, *Anal. Chem.* **2010**, *82*, 5313.
[7] S. Botti, S. Almaviva, L. Cantarini, A. Palucci, A. Puiu, A. Rufoloni, *J. Raman Spectrosc.* **2013**, *44*, 463.
[8] Q. Wan, Q. H. Li, Y. J. Chen, T. H. Wang, X. L. He, J. P. Li, C. L. Lin, *Appl. Phys. Lett.* **2004**, *84*, 3654.
[9] R. Rahmanian, S. A. Mozaffari, *Sens. Actuators, B* **2015**, *207*, 772.
[10] P. C. Chen, S. Sukcharoenchoke, K. Ryu, L. Gomez de Arco, A. Badmaev, C. Wang, C. Zhou, *Adv. Mater.* **2010**, *22*, 1900.
[11] R. Aad, V. Simic, L. Le Cunff, L. Rocha, V. Sallet, C. Sartel, A. Lusson, C. Couteau, G. Lerondel, *Nanoscale* **2013**, *5*, 9176.
[12] a) S. Alnemrat, G. T. Brett, J. P. Hooper, *Appl. Phys. Lett.* **2013**, *103*, 173102; b) J. W. Jaworski, D. Raorane, J. H. Huh, A. Majumdar, S.-W. Lee, *Langmuir* **2008**, *24*, 4938.
[13] A. Kolmakov, M. Moskovits, *Annu. Rev. Mater. Res.* **2004**, *34*, 151.
[14] J. Coey, M. Venkatesan, C. Fitzgerald, *Nat. Mater.* **2005**, *4*, 173.
[15] C. Wang, L. Yin, L. Zhang, D. Xiang, R. Gao, *Sensors* **2010**, *10*, 2088.
[16] a) S. M. Sze, K. K. Ng, *Physics of Semiconductor Devices*, John Wiley & Sons, Hoboken, NJ, **2006**, pp. 200–202; b) B. Zu, B. Lu, Z. Yang, Y. Guo, X. Dou, T. Xu, *J. Phys. Chem. C* **2014**, *118*, 14703.
[17] a) H. Kaftelen, K. Ocakoglu, R. Thomann, S. Tu, S. Weber, E. Erdem, *Phys. Rev. B* **2012**, *86*, 9; b) V. Ischenko, S. Polarz, D. Grote, V. Stavarache, K. Fink, M. Driess, *Adv. Funct. Mater.* **2005**, *15*, 1945.
[18] Y. Engel, R. Elnathan, A. Pevzner, G. Davidi, E. Flaxer, F. Patolsky, *Angew. Chem., Int. Ed.* **2010**, *49*, 6830.
[19] K. Salo, J. Westerlund, P. U. Andersson, C. Nielsen, B. D'Anna, M. Hallquist, *J. Phys. Chem. A* **2011**, *115*, 11671.
[20] A. W. Stelson, J. H. Seinfeld, *Atmos. Environ.* **1982**, *16*, 983.
[21] P. M. Schaber, J. Colson, S. Higgins, D. Thielen, B. Anspach, J. Brauer, *Thermochim. Acta* **2004**, *424*, 131.
[22] J. Coey, K. Wongsaprom, J. Alaria, M. Venkatesan, *J. Phys. D: Appl. Phys.* **2008**, *41*, 134012.
[23] D. Wang, A. Chen, S.-H. Jang, H.-L. Yip, A. K.-Y. Jen, *J. Mater. Chem.* **2011**, *21*, 7269.
[24] Y. Che, X. Yang, G. Liu, C. Yu, H. Ji, J. Zuo, J. Zhao, L. Zang, *J. Am. Chem. Soc.* **2010**, *132*, 5743.
[25] L. Pinnaduwage, T. Thundat, J. Hawk, D. Hedden, P. Britt, E. Houser, S. Stepnowski, R. McGill, D. Bubb, *Sens. Actuators, B* **2004**, *99*, 223.
[26] G. S. Aluri, A. Motayed, A. V. Davydov, V. P. Oleshko, K. A. Bertness, M. V. Rao, *IEEE Sens. J.* **2013**, *13*, 1883.
[27] Z. Yang, X. Dou, S. Zhang, L. Guo, B. Zu, Z. Wu, H. Zeng, *Adv. Funct. Mater.* **2015**, *25*, 4039.
[28] P. A. Pella, *Anal. Chem.* **1976**, *48*, 1632.
[29] R. G. Ewing, M. J. Waltman, D. A. Atkinson, J. W. Grate, P. J. Hotchkiss, *TrAC, Trends Anal. Chem.* **2013**, *42*, 35.
[30] G. He, N. Yan, J. Yang, H. Wang, L. Ding, S. Yin, Y. Fang, *Macromolecules* **2011**, *44*, 4759.

Received: October 15, 2015
Revised: November 28, 2015
Published online: